# 4

# The Approximate Zero IF Receiver Architecture

## 4.1 Introduction

One of the primary goals of this work is to reduce the power consumption of an FM-UWB transceiver. In duty cycled wireless sensor networks the bottleneck is typically the receiver. This is because transmitters only need to be turned on when there is a need to transmit data. As a result their power consumption will only be a small fraction of the overall power consumed by the network. Receivers, on the other hand, need to capture the transmitted data and must therefore be turned on periodically to check whether data is being transmitted. This is why the power consumption of the network will almost entirely be determined by the receiver power consumption. Lowering the duty cycle ratio, or equivalently, increasing the duration of the period between the two on states of the receiver, can be used to bring down network power consumption, but it will also increase latency.

In body area networks, such as [10], where sensors need to provide pressure information from the prosthetic limb to the patient, latency constraints are imposed by the physiological characteristics of the human body. In order to provide a natural sense of touch, the delay from sensors to actuators must not be larger than the time it takes for neurons to convey information from the fingers to the brain. Once the maximum delay limit is reached the only way to reduce network power consumption is to reduce the consumption of the FM-UWB receiver.

Another property that could be of use in the receiver is the capability to handle multiple FM-UWB signals at the same time. This requirement comes from the fact that potentially a large number of sensor nodes may be located close to each other. Providing the multi-user capability would then allow to parallelize data transfer and decrease network delay. Normally, receivers with such capability need good linearity and dynamic range, which again

come at the price of power consumption. If the distance between nodes is not large, and WBAN is a typical example of such an application, sensitivity is not a limiting factor, and can be sacrificed for the benefit of multi-user communication and energy efficiency.

This chapter describes the proposed architecture, intended to further reduce the power consumption of an FM-UWB receiver. Two variations of the architecture are explored, one that aims to provide the multi-user communication capability, and another that attempts to aggressively lower the power consumption, while essentially neglecting all other aspects.

## 4.2 The Uncertain IF Architecture

It is a common observation that in any type of circuits there is a correlation between the frequency of operation and power consumption. The simplest example is the CMOS logic gate, where it can be shown that the dynamic power consumption is proportional to the frequency of operation $P_{dyn} \propto fCV^2$. Similar conclusion holds for other types of circuits, for example, amplifiers typically need more power to achieve the same gain at higher frequencies (or to provide larger bandwidth). As a consequence, the most power-hungry blocks in the receivers are the ones that operate at RF. These are usually the Low Noise Amplifier (LNA), needed to provide a good noise figure, and the frequency synthesizer, where the dominant consumers are the voltage controlled oscillator and frequency dividers. A typical example could be the Bluetooth receiver presented in [1], where the LNA consumes around 25% of the overall power, and 53% of the power is used for the PLL, including the DCO.

Due to the large bandwidth of the FM-UWB signal, precise frequency synthesizers can be completely removed. Gain at high frequencies, however, remains a bottleneck. Consider the FM-UWB receiver from [2], where the LNA consumes 1.6 mW, or 73% of the overall power consumption. A similar case is found in [3], where the LNA consumes 55% of the entire receiver consumption. The preamplifier and the demodulator in the FM-UWB receiver from [4], both operating at RF, consume around 3 mA and 6 mA, respectively. Removing the LNA from the design, or loosening the specifications on RF gain and noise figure, could lead to significant power savings.

The opportunity to decrease power consumption by moving the gain stages from RF to IF was first recognized by Pletcher [5], who demonstrated this approach through the implementation of the "Uncertain IF" receiver. In this design the LNA is merged with the mixer into a single current reuse

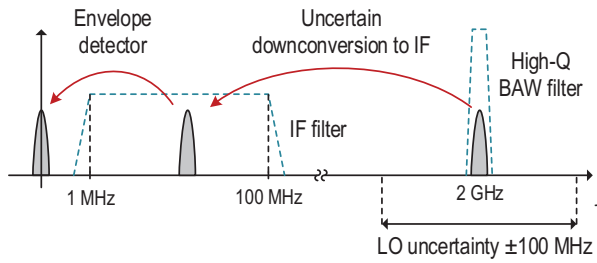


**Figure 4.1** Principle of operation of the uncertain IF receiver.

block, the active mixer. Combined with the external bulk acoustic wave (BAW) resonator, it provides the input matching, and converts the RF signal to IF, where the gain stages are located. The lack of voltage gain at RF simplifies the design and allows for low dc current of the active mixer. Although the power hungry LNA is eliminated from the design, the LO signal must now be generated in order to perform the downconversion. For the proposed design from [5] to be truly power efficient, the LO generator must consume sufficiently low power. A simple three-stage, CMOS ring oscillator used in this design consumes very little power and provides a rail to rail output signal, but this comes at a price. Ring oscillators are generally sensitive to changes in supply voltage and temperature, phase noise is relatively high compared to LC oscillators, and finally the output frequency is rather unstable and tends to drift with time. This is the key point of the architecture from [5]. Instead of using a PLL to stabilize the oscillator frequency, the IF amplifier bandwidth is increased to allow for LO frequency offset. Hence the name "uncertain IF" receiver is used. The described principle is illustrated in Figure 4.1. The designed oscillator generates the LO signal that remains within the $\pm 100$ MHz range from the center frequency. To account for this offset, the IF amplifier is designed with a bandwidth of 100 MHz, assuring that the downconverted signal falls inside the desired band. Using 100 MHz amplifiers to amplify a signal with 10 kHz bandwidth is a necessary overhead, but still results in less power consumed than if a PLL were used to generate the LO signal. The oscillator, however, does need to be calibrated periodically to compensate for the drift due to temperature or supply voltage variation, and maintain the LO frequency within the defined limits. Owing to the fact that these changes are slow, the calibration will only be done once in a few hours, resulting in a negligible overhead in terms of power consunmption. The final stage of the receiver is the envelope detector that demodulates the transmitted OOK (on-off keying) signal. It should still be noted that a relatively good

noise performance in this case was achieved using a narrowband BAW filter that is precisely tuned to the frequency of the transmited signal. Finally, the receiver from [5] reached a power consumption of only 50 $\mu$W, for an input signal at 2 GHz, and is still among the lowest consuming narrowband receivers in the literature today.

The same principle can be applied to the FM-UWB signal. Instead of implementing the wideband amplifiers at RF, the input signal is directly downconverted to zero center frequency using an active mixer (LNA and mixer stack), allowing amplification and processing to be done at low frequencies. Since the LO signal is generated using an imprecise ring oscillator, a certain frequency offset will always be present between the LO signal and the center frequency of the input signal. Hence, the proposed receiver is referred to as the "Approximate Zero IF" receiver. The aforementioned offset should be relatively small compared to the 500 MHz wide input signal, and so the necessary overhead, i.e. larger bandwidth of the IF amplifiers and the demodulator, will be relatively small. Moving the main gain stages from RF to IF results in higher noise figure (NF) of the receiver chain. Since only a limited amount of gain is available at high frequencies, noise of the IF stages will contribute more significantly to the overall noise figure. At the same time, the power consumed by the IF amplifiers can now be greatly reduced since they operate at low frequencies instead of RF, and the same overall gain comes at a lower price.

## 4.3 The Approximate Zero IF Receiver with Quadrature Downconversion

The first proposed receiver architecture is based on a delay line demodulator described in the previous chapter. This demodulator has already been used in some receiver implementations [4, 6]. In its original form it operates directly at RF, and the delay needs to be tuned precisely to the signal center frequency. The demodulator can be moved from RF to baseband, without changing its functionality, if two signal branches are used with a 90° phase shift between them [7]. The two signals can easily be generated by using quadrature LO signals for downconversion.

The proposed receiver architecture is shown in Figure 4.2. Some of the blocks that will be present in the actual implementation are omitted for clarity, and to emphasize functionality. The input signal is directly converted to zero frequency by the mixer. Since a ring oscillator will be used to generate

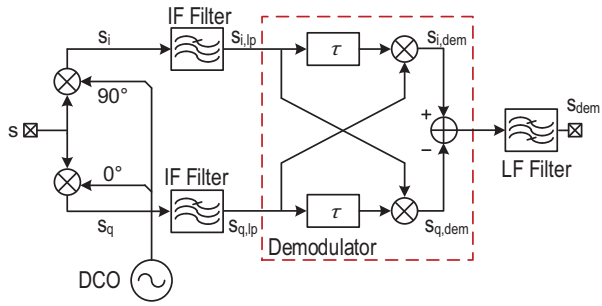


**Figure 4.2** Block diagram of approximate zero IF receiver with IQ downconversion.

the LO signal, some frequency offset will always be present, meaning that the downconverted signal will never be precisely centered at zero, and the architecture is therefore named the "Approximate Zero IF" architecture. The downconverted signal will then be amplified by the IF amplifiers. In Figure 4.2 only filters are shown to emphasize limited bandwidth of the IF path. In this work a 500 MHz wide FM-UWB signal is used. After downconversion, the signal would ideally occupy frequencies from zero to 250 MHz. Accounting for a frequency offset of $\pm$50 MHz, 300 MHz should be sufficient for the bandwidth of the IF path. The case remains the same with the demodulator bandwidth. It needs to be larger in order to accommodate the input signal with a frequency offset.

The principle of operation of the demodulator can be described through the following mathematical model. The simple calculation presented here follows the approach from [8], extending it to account for the LO frequency offset. The aim of the calculation is to explain the principle of operation and provide insights into the main trade-offs when choosing the delay of the demodulator, which is the main design parameter in this case and determines the bandwidth of the demodulator. The FM-UWB signal at the input of the receiver can be represented as:

$$s(t) = A\cos(\omega_c t + \phi(t)), \tag{4.1}$$

where $\omega_c = 2\pi f_c$ is the carrier center frequency of the signal and $\phi(t)$ is the time varying phase, which is the integral of the sub-carrier wave (usually a periodic triangular or sine signal):

$$\phi(t) = \Delta\omega \int_{-\infty}^{t} m(t)\mathrm{d}t. \tag{4.2}$$

The sub-carrier wave $m(t)$ is normalized to the interval [−1,1], and $\Delta\omega$ is the frequency deviation corresponding to half of the FM-UWB signal bandwidth $\Delta\omega = 2\pi\Delta f = \pi B_{UWB}$. The signal is first converted to baseband, such that the signals in the in-phase and quadrature branches are given by

$$s_i(t) = A\cos(\omega_c t + \phi(t))\cos(\omega_{osc} t) \tag{4.3}$$

$$s_q(t) = A\cos(\omega_c t + \phi(t))\sin(\omega_{osc} t) \tag{4.4}$$

where the conversion gain of the mixer is assumed to be unity for simplicity. Note that since the carrier frequency $\omega_c$ does not correspond ideally to the locally generated frequency $\omega_{osc}$, there will be a residual term after mixing that is equal to the difference of the two frequencies. The two filtered, downconverted components at the demodulator input are:

$$s_{i,lp}(t) = \frac{A}{2}\cos(\omega_{off} t + \phi(t)) \tag{4.5}$$

$$s_{q,lp}(t) = -\frac{A}{2}\sin(\omega_{off} t + \phi(t)) \tag{4.6}$$

where $\omega_{off} = 2\pi f_{off} = \omega_c - \omega_{osc}$ is the frequency offset of the LO signal. The two quadrature signals are then multiplied with the delayed copy of each other in the process of demodulation. The signals at the output of the two demodulator mixers are:

$$s_{i,dem}(t) = -\frac{A^2}{4}\cos(\omega_{off}(t-\tau) + \phi(t-\tau))\ \sin(\omega_{off} t + \phi(t)) \tag{4.7}$$

$$s_{q,dem}(t) = -\frac{A^2}{4}\cos(\omega_{off} t + \phi(t))\ \sin(\omega_{off}(t-\tau) + \phi(t-\tau)). \tag{4.8}$$

Finally, the difference of $s_{i,dem}(t)$ and $s_{q,dem}(t)$ results in the following signal:

$$s_{dem}(t) = \frac{A^2}{4}\sin(\omega_{off}\tau + \phi(t) - \phi(t-\tau)). \tag{4.9}$$

Following the same approach as in [8], assuming the time interval $\tau$ is small enough that $\phi(t)$ does not change too significantly, Equation (4.9) can then be approximated by

$$s_{dem}(t) \approx \frac{A^2}{4}\sin(\omega_{off}\tau + \tau\frac{d\phi(t)}{dt}) \tag{4.10}$$

$$= \frac{A^2}{4}\sin(\omega_{off}\tau + \tau\Delta\omega\, m(t)), \tag{4.11}$$

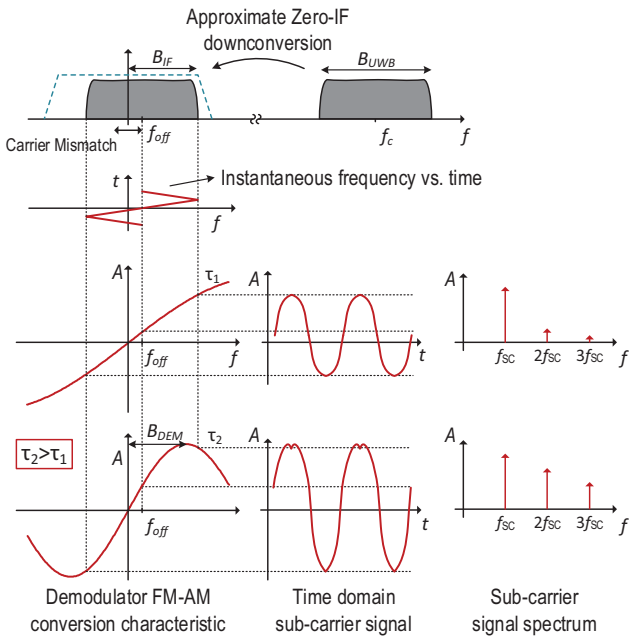


**Figure 4.3** Principle of operation of approximate zero IF receiver with IQ downconversion.

which in fact corresponds to the demodulated signal. The last equation reveals the sinusoidal FM-AM characteristic of the demodulator, showing that it, in fact, acts as a baseband equivalent of the RF delay line demodulator. The illustration of the demodulation principle and the equivalent demodulator characteristic are given in Figure 4.3. The shape of the output demodulated signal is shown for two different values of the delay, assuming that a certain frequency offset is present in the LO signal. The amplitude and the shape of the demodulated signal depend on the demodulator delay $\tau$ and the frequency offset $f_{off}$, as illustrated in Figure 4.3. The demodulator bandwidth can be defined as the monotonic part of the characteristic, i.e. $\tau \times B_{DEM} = \pi/2$. Increasing the delay results in decreased demodulator bandwidth, which increases the amplitude, but also distorts the output signal. Note that unlike with the RF delay line demodulator, the delay $\tau$ is no longer related to the input signal center frequency. Ideally, in the case of the RF delay line demodulator, $\tau$ should be equal to the integer multiple of the quarter period of the center frequency $NT/4$. Any deviation of $\tau$ results in mismatch between the demodulator center frequency and the signal center frequency.

The end effect is equivalent to the LO frequency offset in the approximate zero IF receiver.

The conversion gain is defined as the ratio of the fundamental amplitude of the demodulated signal and the amplitude of the signal at the demodulator input:

$$G_{conv} = \frac{A_{(1)}}{A/2} = \frac{C_1 A^2/4}{A/2} = \frac{A}{2} C_1. \tag{4.12}$$

The coefficient $C_1$ corresponds to the fundamental component of the demodulated signal normalized to $A^2/4$ and accounts for the non-linear characteristic of the demodulator. This coefficient will depend on $\tau$ and $f_{off}$. Assuming a triangular sub-carrier wave, $C_1$ and $C_2$ (normalized second harmonic amplitude) are calculated and plotted in Figure 4.4 as functions of the frequency offset, for several different values of the delay $\tau$. These graphs show the trade-off between the distortion and the conversion gain mentioned above. Choosing larger $\tau$, such that the demodulator bandwidth is smaller than the signal bandwidth, for example $B_{dem} = 200\,\text{MHz}$, will indeed result in a higher gain, but will also make it more sensitive to the carrier offset. For the value of $\tau$ selected to provide 500 MHz bandwidth, the conversion gain is practically half of that obtained for $B_{DEM} = 200\,\text{MHz}$, but remains almost constant even for a very high carrier offset. The conversion gain remains the same for both noise and signal at the input, and in that sense doesn't affect the SNR. However, in a practical realization the demodulator itself will generate noise, and with this noise taken into account higher conversion gain will yield a higher output SNR. It should also be noted that a high demodulator bandwidth (together with IF bandwidth $B_{IF}$) also results in a higher noise bandwidth, which combined with lower gain inevitably leads to a degradation of sensitivity. Looking at the second harmonic, the increase of distortion that comes with the decrease of bandwidth becomes evident. In the ideal case, with no carrier offset, the second harmonic will be zero. However, for the proposed receiver architecture this will never be the case and the amplitude of the second harmonic will depend on offset and demodulator delay. Finally as a compromise between the gain, sensitivity to frequency offset and distortion, a bandwidth of 300 MHz can be chosen for the demodulator implementation and the same value should be used for the bandwidth of the preceding IF amplifiers.

The proposed demodulator can be used to simultaneously demodulate two or more FM-UWB signals. If an additional FM-UWB signal, occupying the

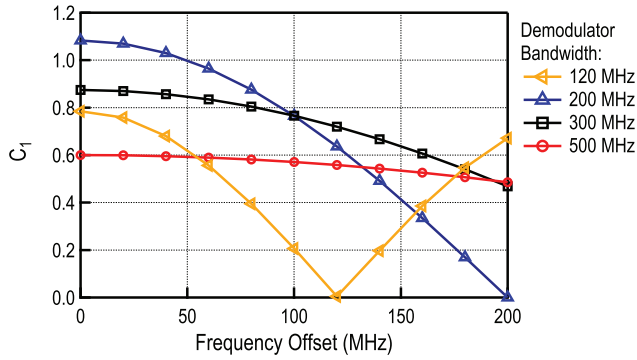


(a)

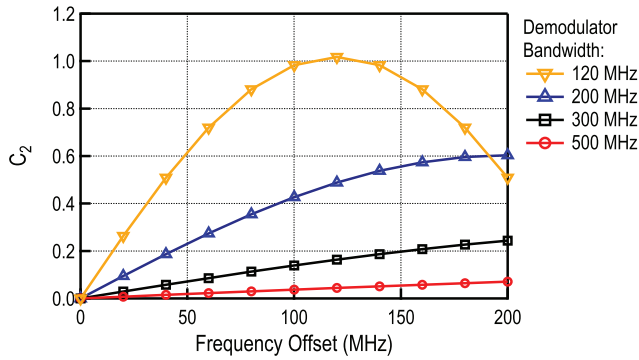


(b)

**Figure 4.4** Normalized fundamental $C_1$ and second harmonic amplitude $C_2$ at the output of the demodulator vs. the offset frequency. First harmonic is proportional to conversion gain. Four curves are plotted for four different values of the demodulator bandwidth (or equivalently different values of the delay $\tau$).

same RF bandwidth but using a different sub-carrier frequency, is present at the input of the receiver, the signals in the I and Q branches are given by

$$s_{i,lp} = \frac{A_1}{2}\cos(\omega_{off}\tau + \phi_1(t)) + \frac{A_2}{2}\cos(\omega_{off}\tau + \phi_2(t)) \tag{4.13}$$

$$s_{q,lp} = -\frac{A_1}{2}\sin(\omega_{off}\tau + \phi_1(t)) - \frac{A_2}{2}\sin(\omega_{off}\tau + \phi_2(t)). \tag{4.14}$$

Following the same steps as in the above calculation the demodulated signal can then be derived as

$$s_{dem} = \frac{A_1^2}{4}\sin(\omega_{off}\tau + \tau\frac{d\phi_1(t)}{dt}) + \frac{A_2^2}{4}\sin(\omega_{off}\tau + \tau\frac{d\phi_2(t)}{dt}) + W(t). \tag{4.15}$$

Aside from the first two terms, which represent the two demodulated signals, an additional term, $W(t)$ appears. This term corresponds to the intermodulation product of the two FM-UWB signals. The effect is the same as for the case of the RF delay line demodulator, where the additional term corrupts the two useful signals and limits the achievable BER. Fortunately, as will be shown, this term will be spread across a large frequency, allowing to filter out most of it in the baseband. The $W(t)$ term is given by

$$\begin{aligned} W(t) = &\frac{A_1A_2}{4}\sin(\omega_{off}\tau + \phi_1(t) - \phi_2(t-\tau)) \\ &+ \frac{A_1A_2}{4}\sin(\omega_{off}\tau + \phi_2(t) - \phi_1(t-\tau)). \end{aligned} \tag{4.16}$$

Using the same approximation as in the single-user case, assuming $\tau$ is very small $W(t)$ can be rewritten as

$$W(t) \approx \frac{A_1A_2}{4}\sin\left(\omega_{off}\tau + \frac{\tau}{2}\frac{d\phi_1(t)}{dt} + \frac{\tau}{2}\frac{d\phi_2(t)}{dt}\right)\sin\left(\phi_1(t) + \phi_2(t)\right) \tag{4.17}$$

$$= \frac{A_1A_2}{2}\sin\left(\omega_{off}\tau + \frac{\tau\Delta\omega}{2}(m_1(t) + m_2(t))\right) \times \sin\left(\Delta\omega\int_{-\infty}^{t}(m_1(t) - m_2(t))\mathrm{d}t\right) \tag{4.18}$$

$$= \frac{A_1A_2}{4}w(t). \tag{4.19}$$

The intermodulation product $W(t)$ consists of two factors. The first one, proportional to the sum of the two sub-carrier signals, is the slow-varying envelope. Clearly the shape of the envelope will depend on the demodulator delay $\tau$, and the frequency offset $f_{off}$, and therefore these two parameters will affect the average power of the intermodulation product. The second

factor is spread from 0 to $2\Delta\omega$, which is equal to the signal bandwidth $B_{UWB}$, with the instantaneous frequency that is proportional to the difference of the two sub-carrier signals. Since the intermodulation product is spread over a very wide band, only a small fraction of its power will fall into the useful sub-carrier band $B_{SC}$. The effect of inter-user interference will be similar to the elevated noise floor at the output of the receiver. This results in a degradation of sensitivity as either the number of users or the power of additional users increase. For a given targeted bit error rate, interference among users will ultimately limit the number of users or the difference in power levels between the two FM-UWB signals that can be handled at the same time.

The average power of the intermodulation product can be calculated as

$$\overline{W(t)^2} = \frac{A_1^2 A_2^2}{16}\overline{w(t)^2} = \frac{A_1^2 A_2^2}{16} C_{MU} \tag{4.20}$$

Factor $C_{MU}$ is the normalized average power of the intermodulation product and depends on $\tau$ and $f_{off}$. It is calculated for two triangular sub-carrier waves and presented in Figure 4.5(a). The decrease of the demodulator bandwidth (increase of $\tau$) in this case leads to increased power of the intermodulation product. Making the approximation that the spectrum of $W(t)$ is flat across the entire band [8], the output signal-to-interference ratio (SIR) can be calculated as

$$SIR_{out} = 10\log_{10}\left(\frac{A_1^2|C_1|^2}{A_2^2 C_{MU}}\frac{B_{UWB}}{B_{SC}}\right), \tag{4.21}$$

where factor $|C_1|^2/C_{MU}$ is added to the original formula from [8] to account for the frequency offset [9]. Figure 4.5(b) shows how this factor changes with the frequency offset for different demodulator bandwidths. As expected the best result is obtained for the highest demodulator bandwidth. The difference is, however, not too significant compared to the case with 300 MHz bandwidth. At the same time, extending the demodulator bandwidth also requires the extension of the IF amplifier bandwidth, which finally leads to increased power consumption. For this reason 300 MHz is chosen as a good trade-off between power and distortion and is the bandwidth that will be used in the receiver implementation described in the following chapter.

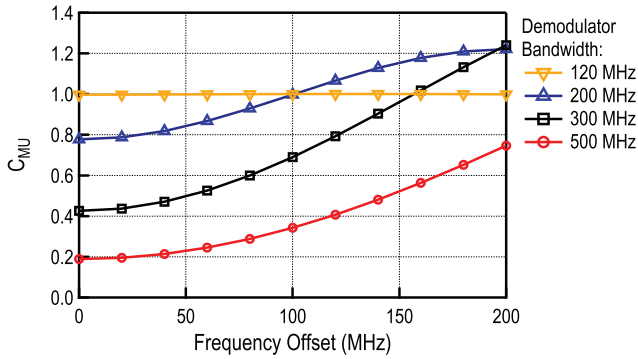


(a)

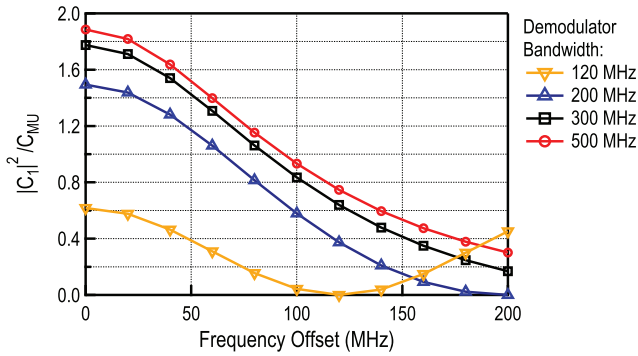


(b)

**Figure 4.5** Coefficient $C_{MU}$ (a) and correction factor $|C_1|^2/C_{MU}$ for SIR (b) as functions of the frequency offset. Four curves are correspond to three different values of the demodulator bandwidth (or equivalently values of the delay $\tau$).

## 4.4 The Approximate Zero IF Receiver with Single-Ended Downconversion

As a general rule, quadrature downconversion is needed in direct downconversion receivers, otherwise part of the information will be lost, and it will be impossible to recover the data. However, because of the properties of the FM-UWB signal, transmitted bits can be recovered even if the signal is directly converted to zero using only a single branch. Shift to a single-ended receiver architecture enables some power savings. First of all, only one IF amplifier can be used, allowing to halve the power of the IF stages. In addition, the

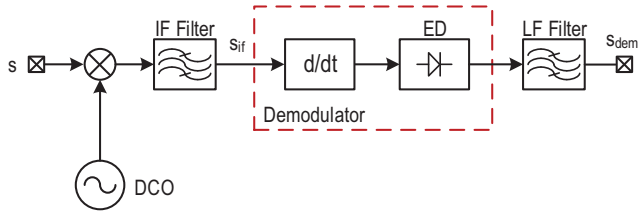


**Figure 4.6** Block diagram of approximate zero IF receiver with single-ended downconversion.

simplified FM demodulator should also allow some savings compared to the IQ delay line demodulator. Finally, the most important savings come from the DCO. Quadrature demodulation requires quadrature LO generation that tends to be power costly. Using a single-ended oscillator simplifies the circuit and allows to reduce power by a factor of more than 2 for the same oscillation frequency.

The operation of the demodulator can be explained using a simplified receiver model, presented in Figure 4.6. Like in the previous case the input FM-UWB signal can be represented as

$$s(t) = A\cos(\omega_c t + \phi(t)), \tag{4.22}$$

where $\phi(t)$ is again the integral of the sub-carrier wave, and $\omega_c$ is the center frequency. After downconversion, the signal at the mixer output is given by

$$s_{mix}(t) = kA\cos(\omega_c t + \phi(t) + \phi_0)\cos(\omega_{osc} t) \tag{4.23}$$

The IF low-pass filter removes all the high frequency components, resulting in the signal at the filter output given by

$$s_{if}(t) = \frac{A}{2}\cos(\omega_{off} t + \phi(t)), \tag{4.24}$$

where $\omega_{off}$ is the offset frequency, that is equal to the difference of the LO frequency and the signal center frequency. The following stage, a differentiator, converts the FM signal into an AM signal given by

$$\frac{ds_{if}(t)}{dt} = \frac{A}{2}\sin(\omega_{off} t + \phi(t))\left(\omega_{off}\tau_0 + \tau_0\frac{d\phi(t)}{dt}\right), \tag{4.25}$$

where $\tau_0$ is the time constant of the differentiator. The resulting signal is then demodulated using the envelope detector. Here, an ideal square law envelope

detector is assumed, resulting in the output signal given by

$$s_{dem}(t) = \frac{A^2}{4}\sin(\omega_{off}t + \phi(t))^2 \left(\omega_{off}\tau_0 + \tau_0\frac{d\phi(t)}{dt}\right)^2$$
$$= \frac{A^2}{8}(1 - \cos(2\omega_{off}t + 2\phi(t)) \left(\omega_{off}\tau_0 + \tau_0\frac{d\phi(t)}{dt}\right)^2 \quad (4.26)$$

The low-pass filter following the envelope detector will practically remove the fast changing component $\cos(2\omega_{off}t + 2\phi(t))$, resulting in the signal at the filter output given by

$$s_{dem}(t) = \frac{A^2}{8}\left(\omega_{off}\tau_0 + \tau_0\frac{d\phi(t)}{dt}\right)^2. \quad (4.27)$$

For simplicity, let us assume that the sub-carrier signal is a sine wave. The demodulated signal is then

$$s_{dem}(t) = \frac{A^2}{8}\left(\omega_{off}\tau_0 + \Delta\omega\tau_0\sin(\omega_{sc}t)\right)^2 \quad (4.28)$$
$$= \frac{A^2}{8}\tau_0^2(\omega_{off}^2 + 2\omega_{off}\Delta\omega\sin(\omega_{sc}t) + \Delta\omega^2\sin^2(\omega_{sc}t)) \quad (4.29)$$
$$= \frac{A^2}{8}\tau_0^2\left(\omega_{off}^2 + 2\omega_{off}\Delta\omega\sin(\omega_{sc}t)\right.$$
$$\left.+\Delta\omega^2\left(\frac{1}{2} - \frac{1}{2}\cos(2\omega_{sc}t)\right)\right). \quad (4.30)$$

In the ideal case the offset frequency is zero, $\omega_{off} = 0$, and the only remaining useful term is the term at twice the sub-carrier frequency

$$s_{dem,2}(t) = \frac{A^2}{16}\Delta\omega^2\tau_0^2\cos(2\omega_{sc}t). \quad (4.31)$$

The demodulation can now be performed using this signal. The same conclusion holds for the triangular wave since it can be represented by the Fourier series, in which case again, the second harmonic of the demodulated sub-carrier wave can be used for the final FSK demodulation. Interestingly, if an ideal differentiator is used and if infinite IF bandwidth is assumed, the amplitude of the second harmonic will be independent of the frequency offset. The first harmonic will appear with the increase of the frequency offset, however in this case, this component can be filtered out by the LF band-pass filter.

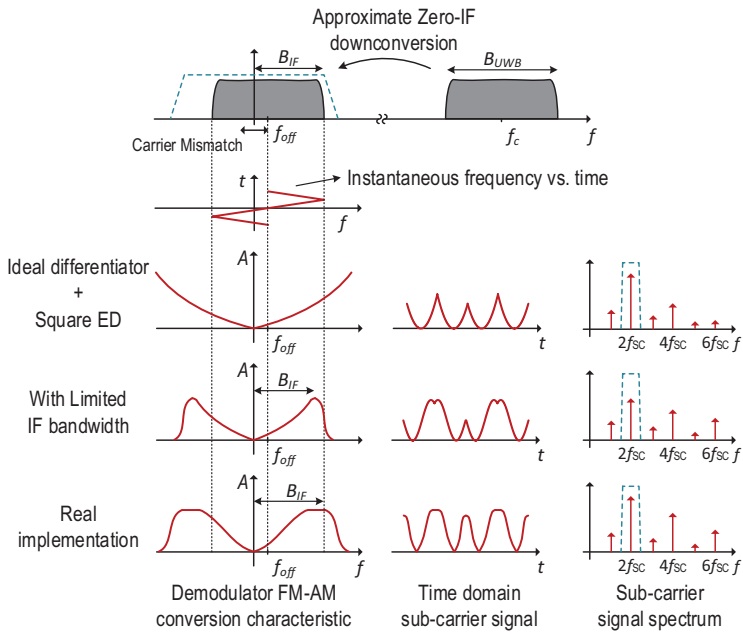


**Figure 4.7** Principle of operation of the approximate zero IF receiver with single-ended downconversion.

The principle of the single-ended baseband FM demodulator is shown in Figure 4.7. In the derivation, an ideal differentiator was used and infinite IF bandwidth was assumed. In a realistic implementation the IF bandwidth will affect the useful signal and will cause the second harmonic of the demodulated signal (used for demodulation) to decrease with frequency offset. Also, the ideal differentiator, used for derivation, will be replaced by a lossy (non-zero dc gain) first order high-pass filter. This filter will have a certain cut-off frequency after which the transfer function flattens. The equivalent FM-AM characteristic should finally resemble the characteristic at the bottom of the Figure 4.7.

The first and second harmonic of the demodulated signal are plotted in Figure 4.8 as functions of the offset frequency. The calculation is done for a triangular sub-carrier signal with varying IF bandwidth. As explained previously, the first harmonic is close to zero for small frequency offsets, and increases as the offset increases. The second harmonic (useful part of the signal), decreases with the frequency offset. This decrease is purely a consequence of the limited demodulator bandwidth, since the second harmonic

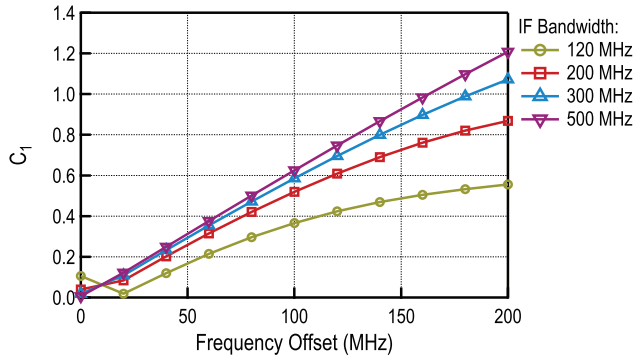


(a)

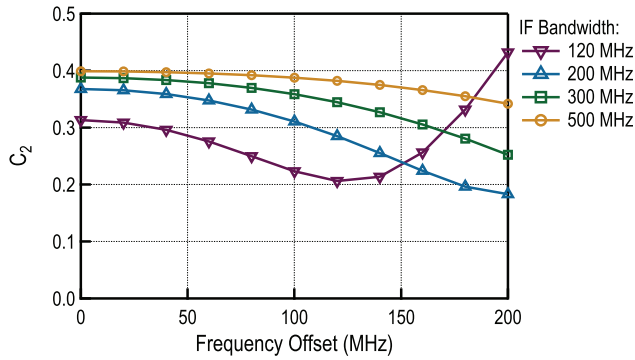


(b)

**Figure 4.8** Normalized fundamental $C_1$ and second harmonic amplitude $C_2$ at the output of the demodulator.

after a perfect square law envelope detector remains constant regardless of the offset. The amplitude of the second harmonic shows less variation with the frequency offset as the IF bandwidth increases. Ideally, the IF bandwidth should then be extended to get the best performance, however this again requires more power for the IF amplifiers, and in the receiver implementation a bandwidth of 300 MHz will be used as a good trade-off.

## 4.5 Receiver Sensitivity Estimation

The first step in estimating the receiver sensitivity is to find the output BER as a function of the SNR at the receiver input. For the approximate zero IF

receiver with quadrature demodulation, the FM-AM conversion characteristic is equivalent to the one of the RF delay line demodulator. The only difference between the two is that the demodulator is located at the baseband instead of RF. The expectation is then that the BER performance of the two receivers remains the same, meaning that the same approximation can be used to estimate the BER. The hypothesis is verified using the high-level model corresponding to the one shown in Figure 4.2. A bandwidth of 300 MHz was used for the IF filters, and 2 MHz for the LF filter that filters the demodulated FSK signal. The bandwidth of the demodulator is chosen larger than the IF bandwidth and is set to aproximately 350 MHz. The simulation results are compared to the Gerrits' approximation [8] in Figure 4.9, using the formula for a non-coherent probability of error. The simulation points match well with the calculated curve, validating the use of Gerrits' approximation for the proposed quadrature receiver.

In the case of the single-ended receiver architecture, the Gerrits' approximation no longer holds in it's original form. However, looking at the receiver structure, after the squaring operation of the envelope detector, the same products appear as in the case of the delay line demodulator. In principle the same approach can be used as in [8], with the difference that the useful signal amplitude is half of the one in the case of the delay line demodulator. The resulting output SNR is then given by

$$\mathrm{SNR}_{\mathrm{out}} = \frac{B_{RF}}{B_{SC}} \frac{(\mathrm{SNR}_{\mathrm{in}}/4)^2}{1 + \mathrm{SNR}_{\mathrm{in}}}. \tag{4.32}$$

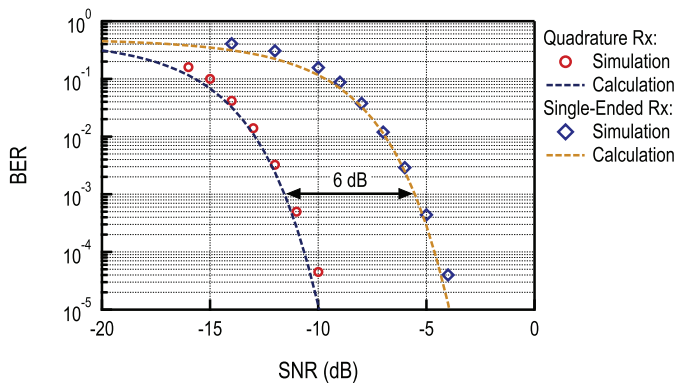


**Figure 4.9** Simulated and calculated BER curves for the approximate zero IF receiver.

The rest of the calculation remains the same as for the delay line demodulator. The resulting calculated BER curve is shifted by approximately 6 dB compared to the BER of the quadrature receiver. This is the price paid for the simplified receiver architecture. The calculated BER curve is compared to the simulated points in Figure 4.9. The used model corresponds to the block diagram of Figure 4.6. The IF bandwidth of 300 MHz was used in the simulation, and a high-pass filter with a cut-of frequency of 300 MHz replaced the differentiator. Such implementation should roughly correspond to the actual implementation of the single-ended receiver.

The two BER curves provide the information on the minimum SNR needed at the receiver input in order to achieve the desired BER. Typically, for low power wireless receivers a BER of $10^{-3}$ is taken as the reference point. The sensitivity of the receiver is then defined as the signal level at the receiver input needed to achieve this BER. To calculate this sensitivity, the noise power at the receiver input must first be calculated. The equivalent input referred noise of the receiver in dBm is given by

$$N = 10\log(\mathrm{k}\mathrm{T}B_{UWB}/1\,\mathrm{mW}) + NF, \tag{4.33}$$

where $NF$ is the noise figure of the receiver, and $10\log(\mathrm{k}\mathrm{T}B_{UWB}/1\,\mathrm{mW})$ is the thermal noise power in dBm at the receiver input at a temperature of $\mathrm{T} = 25°\mathrm{C}$. The used FM-UWB signal bandwidth is $B_{UWB} = 500\,\mathrm{MHz}$. Considering that the main target is to lower the receiver power consumption and that the LNA will be either completely removed, or have very limited performance, relatively high noise figure of the receiver should be accounted for. In [5] the total noise figure of the active mixer and the IF amplifiers is 23 dB. The high noise figure is a consequence of the mixer first architecture and low power gain of the first stage, which results in significant contribution from the IF amplifier. For this design, a 20 dB noise figure will be assumed in order to calculate the achievable sensitivity of the FM-UWB receiver. The sensitivity is then calculated as

$$S_{in} = 10\log(\mathrm{k}\mathrm{T}B_{UWB}/1\,\mathrm{mW}) + NF + \mathrm{SNR}_{min}. \tag{4.34}$$

For the quadrature receiver minimum input $\mathrm{SNR}_{min} = -11.5\,\mathrm{dB}$, which results in a receiver sensitivity of around $\mathrm{S}_{in} = -78.5\,\mathrm{dBm}$. For the single-ended receiver the minimum input SNR is approximately 6 dB higher, which results in sensitivity of $\mathrm{S}_{in} = -72.5\,\mathrm{dBm}$. Achievable sensitivity, although low compared to typical narrowband receivers that achieve levels lower than $-90\,\mathrm{dBm}$ (for example, typical Bluetooth receivers), is sufficient for

communication in body area networks at distances below 1 m. The presented calculation and simulation are valid in an ideal case, where the LO frequency is perfectly aligned with the center frequency of the FM-UWB signal. Since the idea behind power reduction is to use a low quality oscillator whose frequency might drift with time, the sensitivity degradation due to frequency offset should be estimated as well. This is done using the same high-level model, and the results are presented in Figure 4.10.

The 50 MHz offset is taken as a maximum offset that should be tolerated, and the LO frequency must be maintained within these limits. In the practical implementation this will be achieved using a calibration FLL loop

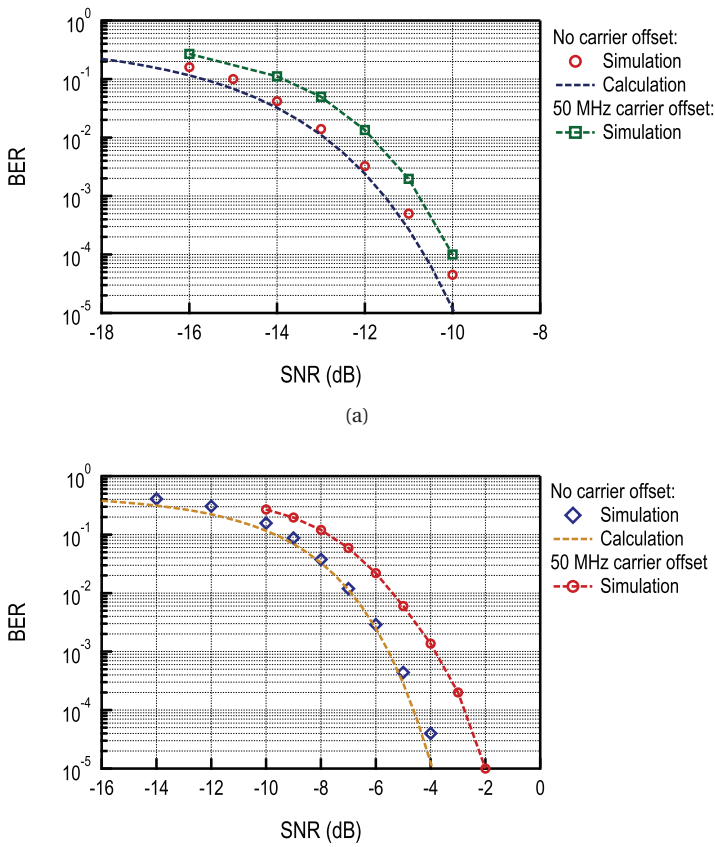


**Figure 4.10** Simulated and calculated BER curves with and without frequency offset for the approximate zero-IF receiver with quadrature downconversion (a) and single-ended downconversion (b).

that is periodically turned on (e.g. by a microcontroller when temperature exceeds certain limits). The sensitivity degradation for a 50 MHz frequency offset and for the receiver with quadrature downconversion is reported in Figure 4.10(a). As can be seen, this degradation is below 1 dB, confirming empirically the initial hypothesis that the frequency offset does not cause a major sensitivity degradation. In the case of the receiver with single-ended downconversion this degradation amounts to around 1.6 dB, as seen in Figure 4.10(b) showing that the simplified architecture is slightly more susceptible to frequency offsets.

It should be noted here that the given calculation and simulation models only account for a noise source at the input of the receiver. The separate contributions of receiver blocks are accounted for through the noise figure, however what is not accounted for is the noise generated by the FM demodulator (delay line demodulator for the quadrature, and envelope detector for the single-ended receiver). Due to the nonlinear nature of FM demodulators, the output noise will depend on the input signal level. In order for the presented sensitivity estimation to be valid, the noise of this block must be negligible compared to the noise from other sources. This requirement is simply achieved by increasing the gain of the stages preceding the demodulator, and it is in fact this requirement that sets a limit for the combined gain of the LNA, mixer and the IF amplifier.

## 4.6 Summary

This chapter presents the general approach to receiver power reduction through use of "uncertain IF" and "approximate zero IF" architectures. The main idea is to loosen constraints on RF stages, that usually consume the most power, and shift the burden to IF where high gain comes at a lower price in terms of power. Two different receiver architectures are proposed. The quadrature approximate zero IF receiver targets to reduce consumption, but also to provide enough linearity to support multi-user communication. Potential to parallelize communication through sub-carrier FDMA, on top of existing TDMA could bring both latency and power savings at a network level. The second architecture, the single-ended FM-UWB receiver architecture, aims solely to reduce power consumption. The used approach sacrifices all other performance aspects in order to provide the lowest possible consumption level, and could be used when there is no need for SC-FDMA. The analysis of the two architectures is presented, providing some insight into

the key points and the principle of operation, together with a short sensitivity analysis that estimates the achievable receiver performance.

The implementation of the concepts presented here is the subject of the following chapters. First, the quadrature approximate zero IF FM-UWB receiver is implemented and characterized standalone. Then, in the second iteration, a full transceiver is integrated. Both receivers are placed on the same die, with the idea to use the single-ended FM-UWB receiver as a low power mode.

## References

[1] A. Sai, H. Okuni, T. T. Ta, S. Kondo, T. Tokairin, M. Furuta, and T. Itakura, "A 5.5 mW ADPLL-based receiver with a hybrid loop interference rejection for BLE application in 65 nm CMOS," *IEEE Journal of Solid-State Circuits*, vol. 51, no. 12, pp. 3125–3136, Dec. 2016.

[2] N. Saputra and J. R. Long, "A short-range low data-rate regenerative FM-UWB receiver," *IEEE Transactions on Microwave Theory and Techniques*, vol. 59, no. 4, pp. 1131–1140, Apr. 2011.

[3] F. Chen, W. Zhang, W. Rhee, J. Kim, D. Kim, and Z. Wang, "A 3.8-mW 3.5-4-GHz regenerative FM-UWB receiver with enhanced linearity by utilizing a wideband LNA and dual bandpass filters," *IEEE Transactions on Microwave Theory and Techniques*, vol. 61, no. 9, pp. 3350–3359, Sep. 2013.

[4] Y. Zhao, Y. Dong, J. F. M. Gerrits, G. van Veenendaal, J. Long, and J. Farserotu, "A short range, low data rate, 7.2 GHz-7.7 GHz FM-UWB receiver front-end," *IEEE Journal of Solid-State Circuits*, vol. 44, no. 7, pp. 1872–1882, July 2009.

[5] N. M. Pletcher, S. Gambini, and J. Rabaey, "A 52 $\mu$W wake-up receiver with $-72$ dBm sensitivity using an uncertain-IF architecture," *IEEE Journal of Solid-State Circuits*, vol. 44, no. 1, pp. 269–280, Jan. 2009.

[6] J. Gerrits, J. Farserotu, and J. Long, "A wideband FM demodulator for a low-complexity FM-UWB receiver," in *The 9th European Conference on Wireless Technology, 2006*, Sep. 2006, pp. 99–102.

[7] M. Kouwenhoven, *High-Performance Frequency-Demodulation Systems*. Delft University Press, 1998.

[8] J. F. M. Gerrits, M. H. L. Kouwenhoven, P. R. van der Meer, J. R. Farserotu, and J. R. Long, "Principles and limitations of ultra-wideband FM communications systems," *EURASIP J. Appl. Signal Process.*, vol. 2005, pp. 382–396, Jan. 2005.

[9] V. Kopta, D. Barras, and C. C. Enz, "An approximate zero IF FM-UWB receiver for high density wireless sensor networks," *IEEE Transactions on Microwave Theory and Techniques*, vol. 65, no. 2, pp. 374–385, Feb. 2017.

[10] J. Farserotu, J. Baborowski, J. D. Decotignie, P. Dallemagne, C. Enz, F. Sebelius, B. Rosen, C. Antfolk, G. Lundborg, A. Björkman, T. Knieling, and P. Gulde, "Smart skin for tactile prosthetics," in *2012 6th International Symposium on Medical Information and Communication Technology (ISMICT)*, Mar. 2012, pp. 1–8.